ACS APPLIED MATERIALS & INTERFACES

www.acsami.org

Research Article

Tetrahedral Framework Nucleic Acids Reestablish Immune Tolerance and Restore Saliva Secretion in a Sjögren's Syndrome Mouse Model

Shaojingya Gao,[†] Yun Wang,[†] Yanjing Li, Dexuan Xiao, Yunfeng Lin, Yu Chen,* and Xiaoxiao Cai*

Cite This: *ACS Appl. Mater. Interfaces* 2021, 13, 42543–42553

Read Online

ACCESS | Metrics & More | Article Recommendations | Supporting Information

ABSTRACT: As one of the most frequent autoimmune diseases, Sjogren's syndrome (SS) is characterized by overactive lymphocytic infiltration in the exocrine glands, with ensuing dry mouth and dry eyes. Unfortunately, so far, there are no appropriate therapies without causing overall immunosuppression. Tetrahedral framework nucleic acids (tFNAs) were regarded as promising nanoscale materials whose immunomodulatory capabilities have already been verified. Herein, we reveal, for the first time, that tFNAs were utilized to treat SS in female nonobese diabetic (NOD) mice, the animal model used for SS. We proved a 250 nM tFNA treatment was successful in suppressing inflammation and stimulating saliva secretion in NOD mice. Specialised proteins for the secretory function and structure of acinar cells in submandibular glands (SMGs) were restored. It has been the permanent goal for SS treatment to establish immune tolerance and stop disease development. Surprisingly, tFNA treatment guided T cells toward regulatory T cells (Tregs), while suppressing T helper (Th) cell responses. Th cells include Th1, Th17, and follicular helper T (Tfh) cells. Tregs are highly significant in immune tolerance. Inducing Tregs is a promising approach to reestablish immune tolerance. Comparable results were also observed in B cell responses. Reductions in the percentage of germinal center (GC) B cells and plasma cells were detected, and a marked increase in the percentage of regulatory B cells (Bregs) was also noticed. The mechanisms of inducing Tregs may associated with cytokine changes. Changes of T cell subsets, especially changes of Tfh, may influence the differentiation of B cells accordingly. Collectively, our results demonstrated the immunomodulatory capacities of tFNAs once again, which may provide a novel, safe, and effective option for the treatment of SS and other autoimmune diseases.

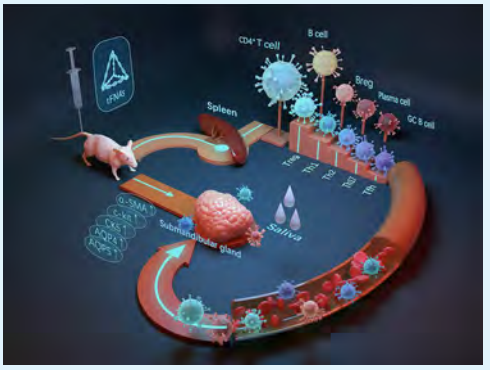

KEYWORDS: *tetrahedral framework nucleic acids, Sjögren's syndrome, saliva secretion, immune tolerance, T cells, B cells*

1. INTRODUCTION

As one of the most frequent autoimmune diseases, Sjögren's syndrome (SS) predominantly affects middle-aged women and the estimated disease prevalence ranges from 0.3 to 3% among the entire population.[1] SS primarily features autoreactive lymphocytes infiltrating exocrine glands, with ensuing oral and ocular dryness.[2,3] Oral dryness predisposes SS patients to caries, loss of teeth, mucosal edema, opportunistic infections, and even loss of the ability to speak and eat.[4,5] Serious quality of life impairments are observed consistently in SS patients. They mainly complain about dysgeusia, dysphagia, and a burning sensation in the mouth, which are typical clinical symptoms closely related to oral dryness.[6,7] Apart from exocrine gland dryness, SS can also lead to systemic manifestations, mainly affecting the skeleton, lungs, kidneys, skin, and peripheral nerves.[8]

SS has received far less research and therapeutic attentions compared with other autoimmune diseases, although it has high prevalence.[2] Currently, the SS management is symptom-based in order to alleviate oral and ocular dryness.[9] The SS patients with systemic manifestations are prescribed systematic immunosuppressive and disease-modifying antirheumatic drugs,[10] which is generally considered as the routine treatment option. However, these drugs can lead to severe side effects such as cancer and life-threatening infections because of their broad immunosuppression These treatments unfortunately do not address the etiological factor of SS.[11] The optimal way for SS management should be more precise depending on thorough understanding of the immunopathological mechanisms involved.

Lymphocytic infiltration of exocrine glands is the iconic histological feature of SS. In salivary glands (SG), the

Received: August 4, 2021
Accepted: August 25, 2021
Published: September 3, 2021

https://doi.org/10.1021/acsami.1c14861
ACS Appl. Mater. Interfaces 2021, 13, 42543–42553

dominant infiltrated lymphocytes are mainly $CD4^+$ T cells and B cells. Specifically, there are 15−50% $CD4^+$ T cells and 20−60% B cells.[3,12,13] In SS, $CD4^+$ T cells mostly consist of T helper (Th) cells and regulatory T cells (Tregs), and Th cells include Th1, Th2, Th17, and follicular helper T cells (Tfh)[2]. Th1 mainly secretes IFN-γ to activate macrophages. IFN-γ is overproduced in the salivary glands and peripheral blood of SS patients, compared with normal population.[14] Overall, the balance between Th1 and Th2 is influenced by the stage of the disease. In SS, an increased IL-17 level and its mRNA expression in salivary glands have been detected.[15] As IL-17-producing T cells, Th17 plays a considerable role in pathogenic mechanism of SS.[16] Tfh and the secretion of IL-21 lead to the formation of germinal center-like structures that induce B cell activation.[12] Th2 and Th17 cells can also participate in activating B cells.[17] Overactive $CD4^+$ T cells and B cells are the most common biological sign of SS. However, among $CD4^+$ T cell and B cell subsets, regulatory B cells (Bregs) and Tregs are considered to suppress the excessive cell activities and maintain immune tolerance.[18] In SS, the percentage of Bregs and Tregs dropping in blood and salivary gland has been demonstrated.[19,20] Therefore, one of the optimal ways to manage SS is immunotherapies. Immunotherapies may reestablish immune tolerance through inducing Bregs and Tregs, preventing the overactive immune cells and halting the progress of SS.[9]

However, immunotherapies for SS are constrained to a few patients, due to the scant options of therapeutic materials. Many defects of traditional therapeutic materials lead to their limited application, consisting of short half-life period, in vivo instability, unexpected bioactivity and tissue toxicity.[21,22] On the basis of the outstanding capability to target immune cells and signals precisely, nanoscale materials are paving its way into the field of immunotherapy at an unprecedented speed.[23−25] As the promising nanoscale materials, a huge range of DNA nanostructures have been widely applied in immunotherapies.[26−28] In most cases, these DNA nanostructures cannot regulate the immune system by themselves.[24,29,30] These DNA nanostructures are generally regarded as nanocarriers to transport small therapeutic agents to areas of the body that are otherwise too difficult to reach.[22,31] However, tetrahedral framework nucleic acids (tFNAs), as one of the most hopeful DNA nano materials, are especially dramatic in a large range of biological research fields.[32−36] Notably, recent studies verified that tFNAs could travel through the cell membrane of macrophages, stimulate macrophage activation, and induce M1 polarization.[37] These indicated that tFNAs may be a potential therapeutic material option for immunotherapies in autoimmune diseases.

Herein, the immunomodulatory capacities of tFNAs in managing SS have been verified. Female nonobese diabetic (NOD) mice are adopted in our study, as the animal model of SS. We find that tFNAs successfully reestablish immune tolerance through particularly suppressing overactive immune cells and inducing regulatory immune cells. tFNAs can protect the salivary glands from lymphocytic infiltration and preserve the tissue structures and functions. So far, our study results demonstrate the viability, security, and availability of tFNA treating SS via reestablishing immune tolerance and restoring saliva secretion of SS.

2. MATERIALS AND METHODS

2.1. Synthesis and Characterization of tFNAs. The synthetic steps of synthesizing. tFNAs agree with the previous studies[37−39] To demonstrate the successful synthesis of tFNAs, the measurements were performed similar to previous study.[40−42] High-performance capillary electrophoresis (HPCE, Bioptic, Qsep100, Taiwan) and 8% polyacrylamide gel electrophoresis (PAGE) were both utilized to determine the molecular weights of ssDNA and tFNAs. Atomic force microscopy (AFM, SPM-9700 Instrument; Shimadzu, Kyoto, Japan) and transmission electron microscopy (TEM, Hitachi HT7700, Tokyo, Japan) were utilized to verify the morphology of tFNAs. Zeta potential and the average size of tFNAs were examined by a Zetasizer Nano ZS90 (Malvern Instrument Ltd., Malvern, UK).

2.2. Mice. NOD/ShiLtJ mice served as the SS diseased animal model, whereas ICR mice served as the normal mice. Female NOD and ICR mice aged 11 weeks were purchased from Jiangsu GemPharmatech Co, Ltd. Mice were housed in a specific pathogen-free animal facility, with unrestricted access to standard water and diet. The weight of the mice was about 25 g. Ethics committee of Sichuan University approved all animal-related procedures. Group 1, Normal mice: ICR mice. Thirty female NOD mice were randomly divided into three groups equally. Group 2, NOD + Saline: NOD mice treated with normal saline. Group 3, NOD + T250: NOD mice treated with 100 μL of 250 nM tFNAs (dissolved in normal saline). Group 4, NOD + T500: NOD mice treated with 100 μL of 500 nM tFNAs (dissolved in normal saline). tFNAs and normal saline were given to each mouse by tail-vein injection every other day for consecutively 4 weeks. Mice at 20, 25, and 30 weeks of age were euthanized using Zoletil50 (Virbic, France) followed by eyeball exsanguination, respectively. Peripheral blood (PB), spleen, heart, lung, kidney, and submandibular gland (SMG) samples were collected for the experiments described below.

2.3. Measurements of Stimulated Saliva Flow Rate (SFR). The procedures of measurements of SFR are consistent with previous studies.[19] SFR was measured at 12 weeks of age (pretreatment), then at 15, 18, 21, 24, 27, and 30 weeks of age.

2.4. Histologic Analysis. Heart, spleen, lung, kidney, and SMG samples were collected in paraformaldehyde. Then, tissues were embedded with paraffin and sliced into sections. The sections were dyed with hematoxylin and eosin (H&E). The sections of SMGs were scored to assess the degree of lymphocytic infiltration, according to previous research.[15] The focus score corresponded to the number of foci where more than 50 lymphocytes infiltrate. The focus area was the area occupied by more than 50 lymphocytes. The ratio index was determined as the percentage of the focus area to the total area of the SMGs, as analyzed by *ImageJ* software (National Institutes of Health, Bethesda, MD, USA).[15]

2.5. Enzyme-Linked Immunosorbent Assay (ELISA). The SMG and serum levels of IFN-γ, TGF-β, IL-10, IL-17, and IL-21 were quantified with commercial ELISA kits (Meimian Biology, Wuhan, China), following the instructions.

2.6. Immunofluorescence. SMG frozen sections were prepared. Sections were stained with anti-aquaporin 4 (AQP4), anti-aquaporin 5 (AQP5), anti-cytokeratin 5 (CK5), antialpha smooth muscle actin (α-SMA), anti-c-kit, anti-CD4, anti-B220, anti-BAFF, anti-Ki67, and deoxynucleotidyl TdT-mediated dUTP nick-end labeling (TUNEL, Servicebio, Wuhan, China) as the primary antibodies. Polyclonal donkey antimouse secondary antibodies (Servicebio, Wuhan, China) were employed for 1 h at room temperature. Finally, DAPI (Servicebio, Wuhan, China) was employed for 3 min. The percentage of stain-positive area to total area of the section was calculated by *ImageJ* software.

2.7. Flow Cytometry. Mouse lymphocytes were isolated from the PB, the spleen, and SMGs of normal mice and NOD mice. For $CD4^+$ T cells, surface protein and intercellular protein were both stained. The fluorochrome-labeled surface mAbs were employed, including CD4 APC-Cy7 (BD Bioscience), CD25 PE-Cy7 (BD Bioscience), PE-Cy7 CXCL5 (BD Bioscience), and BB700 PD-1 (BD Bioscience). Lymphocytes were strained with these fluorochrome-labeled surface mAbs at 4 °C for 30 min. Intracellular proteins were dyed with the fluorochrome-labeled intracellular mAbs, including IFN-γ 847 (BD Bioscience), transcription factor forkhead box P3 (Foxp3) Alexa Fluor 488 (eBioscience), IL-4 PE (BD Bioscience), and IL-17 PerCP-Cy5.5

https://doi.org/10.1021/acsami.1c14861
ACS Appl. Mater. Interfaces 2021, 13, 42543−42553

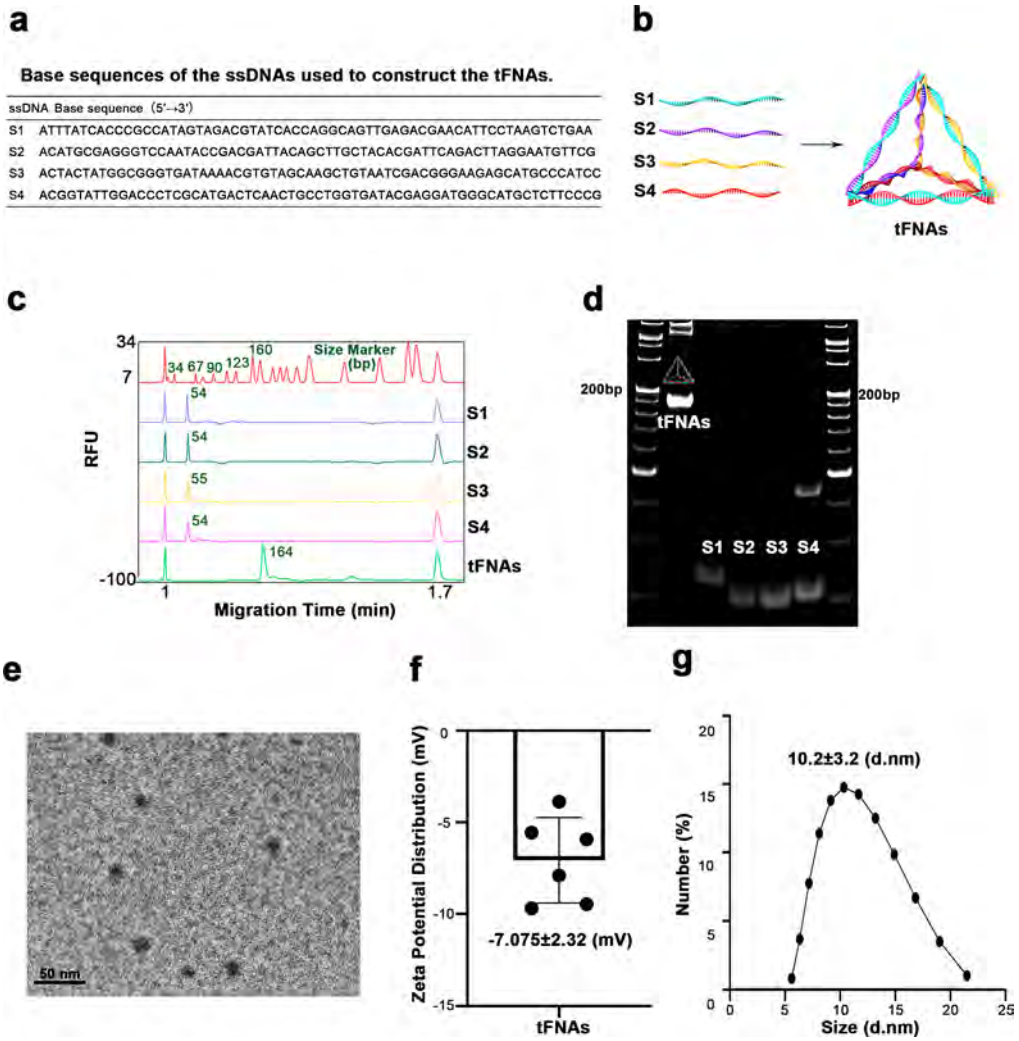

Figure 1. Characterization of tFNAs. (a) Base sequences of the ssDNAs used to construct the tFNAs. (b) Schematic diagram of tFNAs. (c, d) Theoretical molecular weight of synthesized tFNAs was verified by HPCE and 8% PAGE. The results demonstrated successful synthesis of tFNAs. (e) Morphological characteristics of synthesized tFNAs were demonstrated by TEM. (f) Zeta potential and (g) size of synthesized tFNAs. Data are presented as mean ± SD.

(BD Bioscience) and at 4 °C for 40 min. For B cells, the lymphocytes were stained with BB515 CD19 (BD Bioscience), APC B220 (BD Bioscience), BV605 CD1d (BD Bioscience), BV421 CD95 (BD Bioscience), APC-R700 CD5 (BD Bioscience), PE CD138 (BD Bioscience) and PE-Cy7 GL7 (BD Bioscience) 4 °C for 30 min. The stained lymphocytes were assessed via Attune Nxt Flow Cytometer (Thermo Fisher, USA) and *FlowJo* software version 10 (BD Bioscience). To stain intracellular protein, we stimulated the lymphocytes with phorbol 12-myristate 13-acetate (100 ng/mL; Sigma), brefeldin A (1 mg/mL; Sigma), and ionomycin (1 mg/mL; Sigma) at 37 °C for 6 h and then incubated them with FITC-conjugated anti-CD4 antibody (BD Bioscience). Th1, Th2, Th17, Tfh, and Treg cells were stained with the fluorochrome-labeled surface mAbs. Cells were then fixed, permeabilized, and washed using a BD Cytofix/Cytoperm Kit.

2.8. Statistical Analysis. *Graphpad Prism 8* was utilized to perform the data analysis and draw the graphs. All data were presented as mean ± SD or as percentages. All data were analyzed with one-way analysis of variance (ANOVA). A confidence level of 95% was considered significant. For all tests, statistical significance of p value is shown as *, $P < 0.05$, **; $P < 0.01$; ***, $P < 0.001$; or not significant $P > 0.05$.

3. RESULTS AND DISCUSSIONS

3.1. Synthesis and Characterization of tFNAs. Four ssDNAs of equimolar amount paired tFNAs in the bases of complementary matching principle (Figure 1a). The diagrammatic drawing shows the fabrication of tFNAs (Figure 1b). HPCE and 8% PAGE were employed to demonstrate tFNAs were successfully synthesized. (Figure 1c, d). According to the markers in HPCE and 8% PAGE, the molecular weight of tFNAs was about 200 bp, which was consistent with the value in previous study[39,40] (Figure 1c, d). AFM and TEM were conducted to observe the shape of tFNAs, which was like a triangle (Figure 1e, Figure S1). Moreover, tFNAs had a charged surface of −7.075 ± 2.32 mV and the average size of tFNAs was 10 nm. (Figure 1f, g)

3.2. tFNAs Alleviates SS in NOD Mice. In female NOD mice, SS-like disorders normally emerge at age of 7 weeks. For 12-week-old female NOD mice, SS is at the fully developed stage. Therefore, 12-week-old female NOD mice were employed in the study.[43,44] tFNA treatment was conducted for 4 weeks and followed until NOD mice reached the age of 30 weeks (Figure 2a). Lymphocytic infiltration of salivary glands is the classic histological feature of SS. The severity of

https://doi.org/10.1021/acsami.1c14861
ACS Appl. Mater. Interfaces 2021, 13, 42543−42553

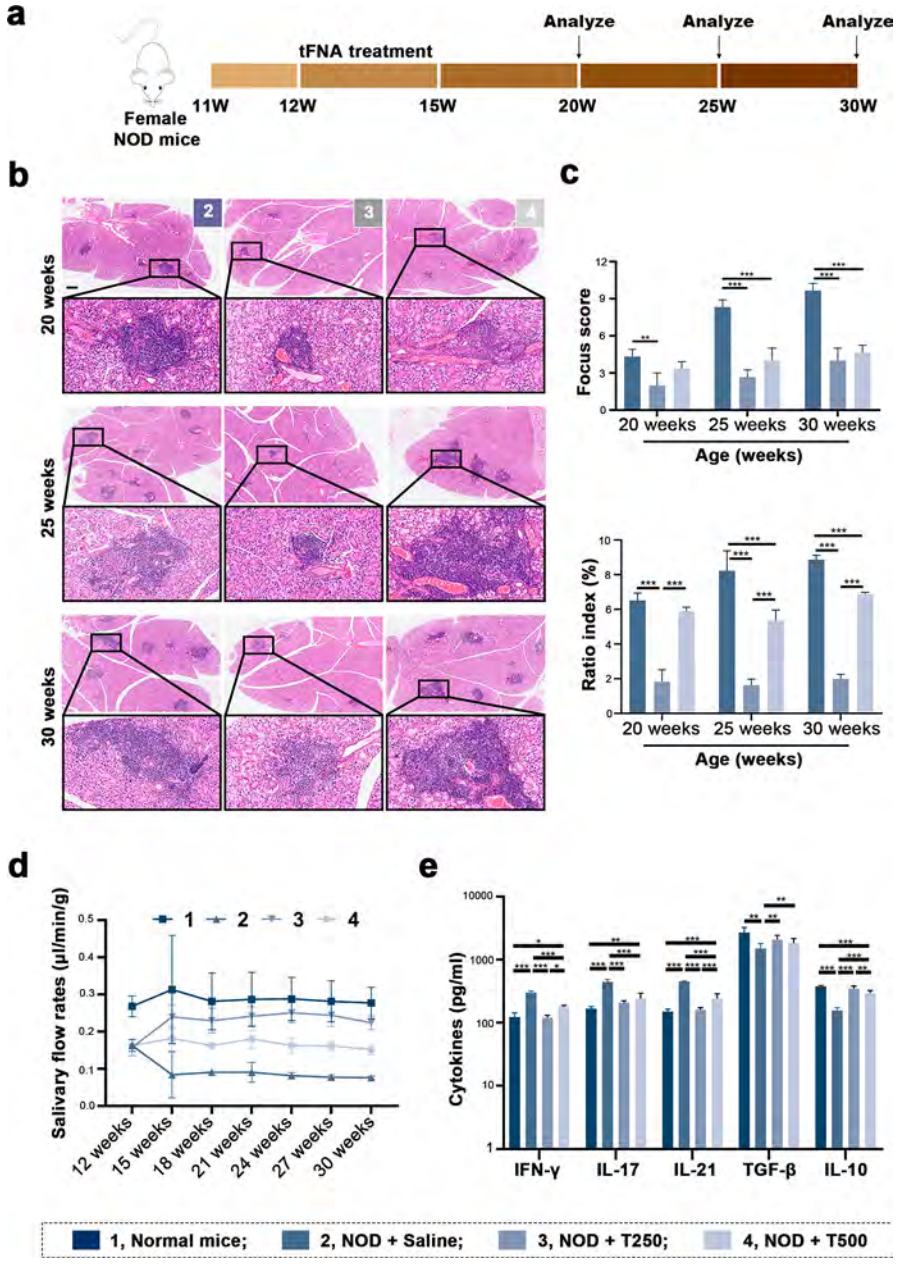

Figure 2. tFNAs protected the SMGs from the inflammatory damage and improved the salivary function in NOD mice. (a) Experimental scheme. (b) Representative histological images (from three or four mice in each group at each time point) showing lymphocytic infiltration in the SMGs of 20-, 25-, and 30-week-old mice (scale bar: 200 μm). (c) Degree of lymphocytic infiltration in the SMGs was analyzed by the focus score and the ratio index. Focus area was the area occupied by lymphocytic infiltrates ($\geq$50 lymphocytes). The ratio index was defined as the percentage of the focus area to the total area. (d) SFR of NOD mice measured every 3 weeks throughout the experiment. SFR was determined by volume of saliva/(min g of body weight). (e) Expression levels of pro- and anti-inflammatory cytokines in SMGs of 30-week-old mice (from four mice in each group) were detected by ELISA kits. Throughout, data are presented as mean $\pm$ SD *, $p < 0.05$, **, $p < 0.01$, ***, $p < 0.001$. Statistical analyses were performed using one-way ANOVA.

the lymphocytic infiltration was assessed by H&E-staining of SMG sections. Focus score (the number of the focus of lymphocytic infiltrates) and ratio index (the percentage of the focus area to the total area) were employed to further analysis. Both NOD + T250 and NOD + T500 groups demonstrated lower focus scores compared with the NOD + saline group, whereas the NOD + T250 group had the smallest ratio index among all three treatment groups (Figure 2b, c).

SFR is a commonly used indicator for the function of salivary glands as well as a significant tool to evaluate of the treatment effects. Because of this parameter, the salivary secretion of 12-week-old NOD mice was already lost partially, which is consistent with the disease onset time of Sjogren's syndrome reported in the literature[43,44] (Figure 2d). Comparatively, there was no marked differences in SPR between the NOD + T250 group and the normal mouse group, and the trend continued until the end of follow-up. However, there was a significant difference between the NOD + T500 group and the normal mouse group. The result of SPR indicated that the treatment of 250 nM tFNAs was effective in restoring saliva secretion of the salivary glands in NOD mice.

https://doi.org/10.1021/acsami.1c14861
ACS Appl. Mater. Interfaces 2021, 13, 42543−42553

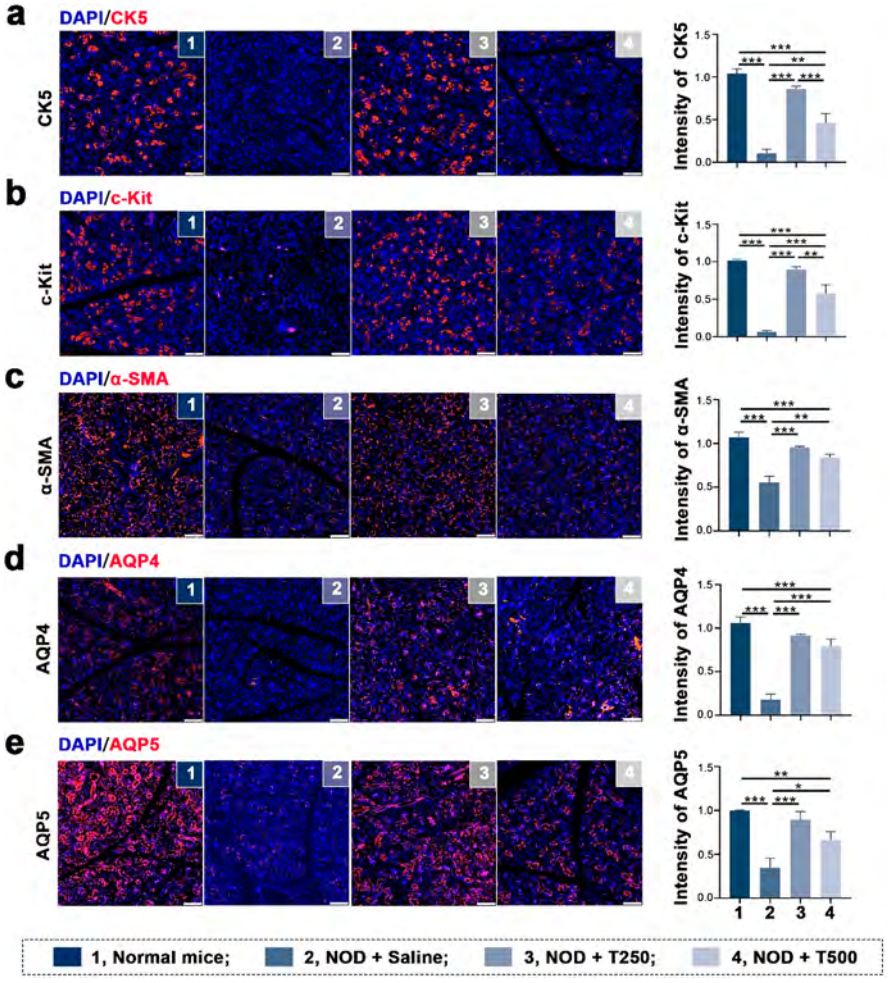

Figure 3. tFNAs preserved the specific cells in the SMGs. Specialized cell subpopulations of 30-week-old mice (from four mice in each group) were analyzed by immunofluorescence staining. (a–e) Representative immunofluorescence images stained for CK5, c-Kit, α-SMA, AQP4, and AQP5, respectively (scale bar: 100 μm) and quantitative analysis. Throughout, data is presented by mean ± SD *, $p < 0.05$, **, $p < 0.01$, ***, $p < 0.001$. Statistical analyses were performed using one-way ANOVA.

Furthermore, tFNA treatment affected the level of various proinflammatory cytokines and anti-inflammatory cytokines simultaneously in the serum and the SMGs of NOD mice. As important anti-inflammatory cytokines, TGF-β and IL-10 are significant in suppressing overactive immune cells. We found that the levels of these anti-inflammatory cytokines increased both in the PB and the SMGs after tFNA treatment (Figure 2e, Figure S2). IFN-γ, IL-17, and TNF-α, regarded as proinflammatory cytokines, decreased in the NOD + T250 and NOD + T500 groups, respectively. These results indicated that tFNA treatment, especially tFNAs at 250 nM, had an apparent anti-inflammation effect and helped restore saliva secretion of the SG in NOD mice throughout the follow-up period.

3.3. tFNAs Preserve Specific Cells in SMGs. To explore the protective effect of tFNA treatment, we evaluated several markers related to saliva secretion, gland formation, and gland regeneration in SMGs by immunofluorescence staining. The expressions of several specific proteins in SMGs were analyzed, including, CK5, c-Kit, and α-SMA, as they are crucial to maintaining the normal structure of SMGs. These specific proteins are specific markers for ductal cells, progenitor cells, and myoepithelial cells, respectively. We noticed that in the NOD + saline group, the SMGs showed a weak staining for the expression of these specialized markers (Figure 3a–c). However, when mice were treated with 250 nM tFNAs, these specific proteins became highly expressed in the SMGs. AQPs closely related to saliva secretion are they are water-permeable channels proteins. Among AQPs, AQP4 located in acinar and ductal cells and AQP5 is predominantly detected in acinar cells of SG. These two proteins alter markedly in SS.[45] After tFNA treatment, we detected many more cells positive for AQP4 and AQP5 in the NOD + T250 group (Figure 3d, e).

AQP4 and AQP5 are water channel proteins, which are closely associated with the production of saliva and tears. A large number of studies supported the view that AQPs were one of the crucial factors related to oral dryness resulting from SS. It therefore could be inferred that AQPs involved in SS were must-achieve therapeutic targets in effective disease therapy.[45] In normal mice, AQP4 could be detected at the basal membrane of SG acinar and ductal cells, and AQP5 was predominantly located at apical membranes of SG acinar cells. The modification in the AQP5 position has been well confirmed in NOD mice, known as the SS animal model.[46] In contrast to its normal apical localization, AQP5 was reported to relocate at basolateral membranes in SS. Apart from a change in localization, the expression levels of these specialized proteins were also significantly lowered in SS

https://doi.org/10.1021/acsami.1c14861
ACS Appl. Mater. Interfaces 2021, 13, 42543–42553

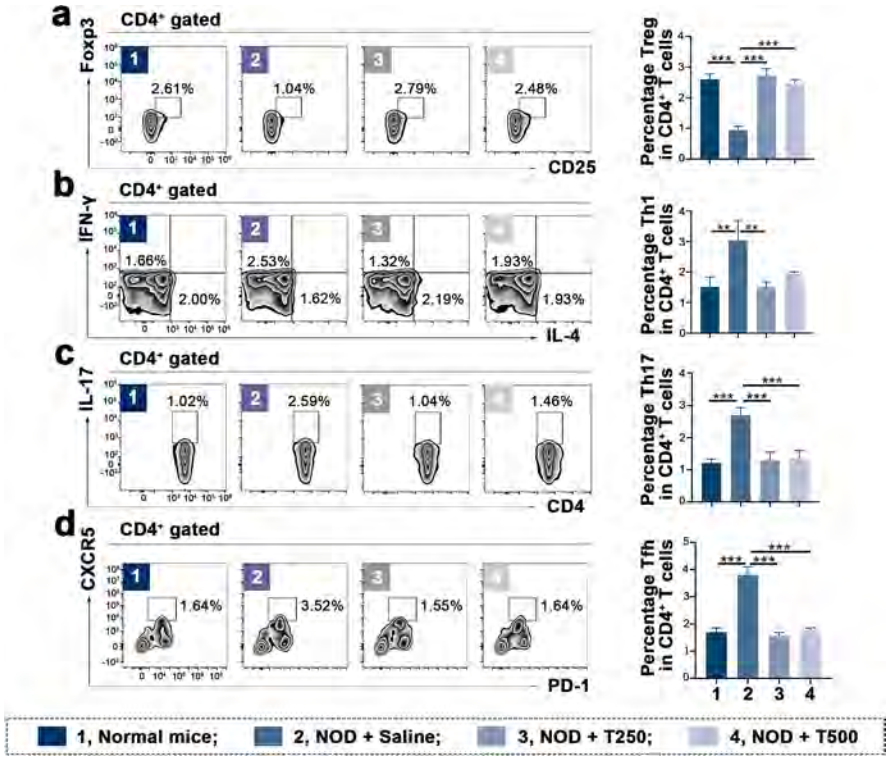

Figure 4. tFNAs regulated T cell responses in the SMGs of 30-week-old NOD mice. (a) Representative flow cytometry pattern and quantitative analyses of $CD4^+CD25^+Foxp3^+$ T cells (Tregs) obtained from the SMGs (from four mice in each group). (b) Representative flow cytometry pattern and quantitative analyses of $CD4^+IFN\gamma^+$ T cells (Th1) and $CD4^+IL4^+$ T cells (Th2) obtained from the SMGs (from four mice in each group). (c, d) Representative flow cytometry pattern and quantitative analyses of $CD4^+IL17^+$ T cells (Th17) and $CD4^+PD\text{-}1^+CXCR5^+$ T cells (Tfh) obtained from the SMGs (from four mice in each group). Throughout, data are presented as mean ± SD *, $p < 0.05$, **, $p < 0.01$, ***, $p < 0.001$. Statistical analyses were performed using one-way ANOVA.

because of the inflammatory destruction of salivary gland structure. Fortunately, the tFNA-treated groups showed higher immunofluorescence intensity of the specialized proteins. These upregulations in the tFNA-treated mice well explained the SFR detection results.

The causal factor directly responsible for the AQP5 relocation and declining expression levels of specialized proteins in SS was inflammatory cytokines in SG.[47] For NOD mice and SS patients, a number of proinflammatory cytokines were upregulated in both the PB and the SMGs.[15] At the early stage of SS, overexpressed IFN-γ and IL-17 were the dominant cytokines in the SMGs and the PB,[48] mainly produced by Th1 and Th17, respectively. This could serve as the sound evidence that T cells were the vital mediators at the early stage of SS, helping with creating the inflammatory microenvironment in vivo.[49] In the NOD + saline group, the levels of IL-21 were remarkably increased in the PB and the SMGs, which was supposed to be strongly associated with Tfh activities that manipulate B cell migration and differentiation.[12] Thus, these proinflammatory cytokines and overactive cells were long regarded as specific therapeutic targets for SS. In terms of Tregs, Treg cells are a special subgroup of $CD4^+$ T cells that perform essential functions and exert their suppressive activity partially by the controlled release of proinflammatory cytokines. IL-10, mainly produced by Tregs, suppressed the effector immune responses and delayed the differentiation of B cells. For anti-inflammation in SS, nonsteroidal anti-inflammatory drugs, hydroxychloroquine, methotrexate, and glucocorticoids were regularly used in the clinical setting. However, there was little or no solid evidence for their effectiveness.[50] The majority of these drugs were broad-spectrum immunosuppressive drugs that could not carry out precise immune regulation and modulation, frequently resulting in miscellaneous side effects. Unlike these immunosuppressive drugs, tFNA treatment achieved the goal of anti-inflammation by favoring anti-inflammatory cytokines while inhibiting proinflammatory cytokines. Cell proliferation and cell death were detected by immunofluorescence stained with Ki67 and TUNEL in SMGs at 15 weeks post-treatment. Compared to the NOD + saline group, the cell proliferation rate was significantly higher and the cell death rate was significantly lower in the NOD + T250 group, statistically (Figure S3).

3.4. tFNAs Regulate $CD4^+$ T-cell Differentiation. The ultimate goal of the SS therapy is to suppress overactive immune cells and induce regulatory immune cells to reestablish immune tolerance. We investigated how tFNA treatment directed $CD4^+$ T-cell responses in the PB, the spleen, and the SMGs at 15 weeks post-treatment by immunofluorescence staining and flow cytometry. Plenty of T cells, including $CD4^+$ and $CD8^+$ T cells, infiltrating the SMGs were found in the NOD + saline group at the end point (Figures S4 and S5). In the NOD + T250 group, a reduction in the accumulative frequency of $CD4^+$ T cells in the SMGs was detected, indicating the alleviated overall inflammation.

Among $CD4^+$ T cell subsets, Tregs, featured by transcription factor Foxp3, play a pivotal role in maintaining immune tolerance.[49,51] In the NOD + saline group, the frequencies of Treg cells in the PB, the spleen, and the SMGs were much less than those in the normal mouse group (Figure 4a, Figures S6

https://doi.org/10.1021/acsami.1c14861
ACS Appl. Mater. Interfaces 2021, 13, 42543−42553

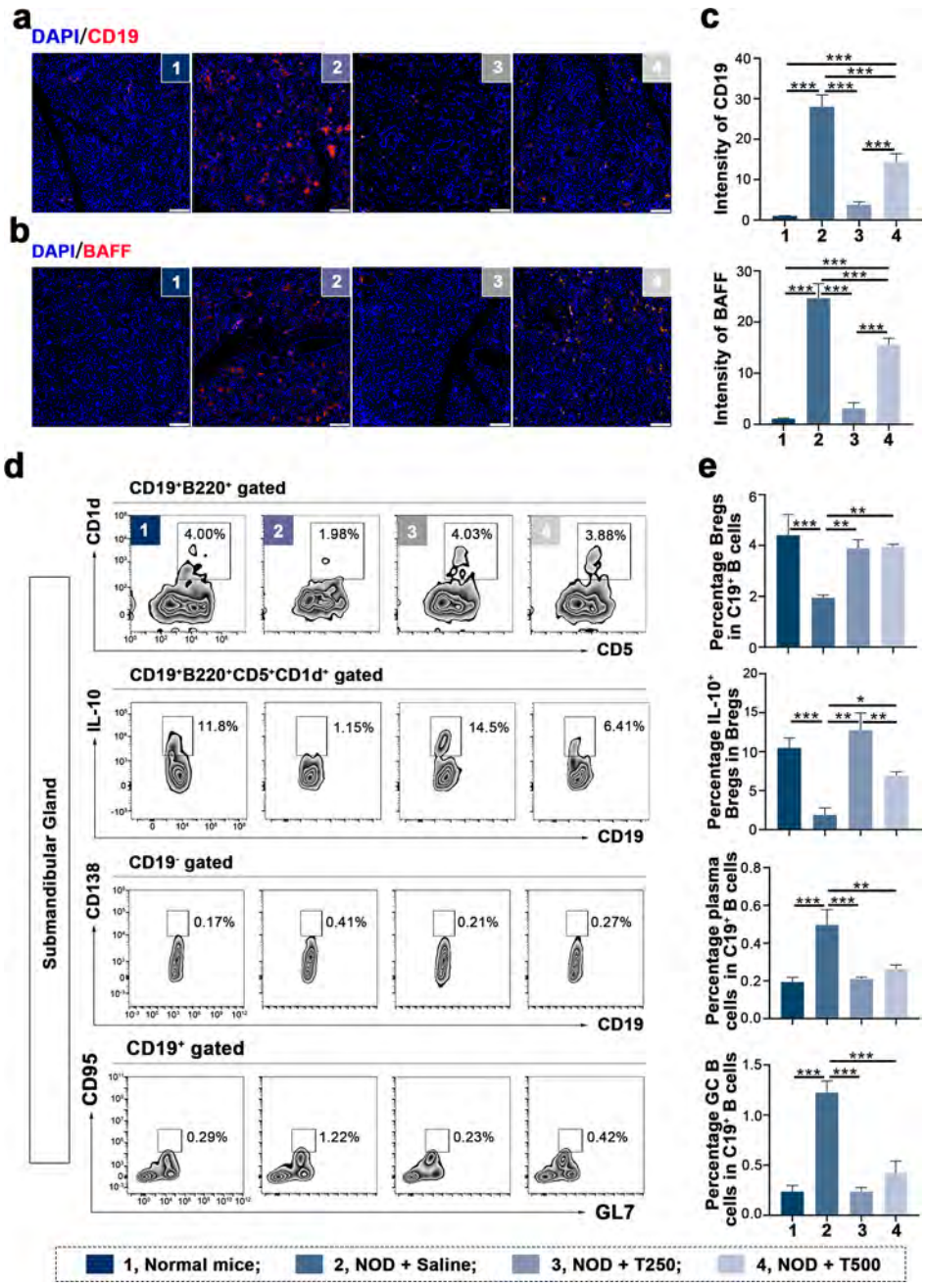

Figure 5. tFNA therapy regulated B cell responses in 30-week-old NOD mice. (a–c) Representative immunofluorescence images of the SMGs (from four mice in each group) stained for CD19 and BAFF (scale bar = 100 μm) and quantitative analysis. (d) Representative flow cytometry pattern of $CD19^+B220^+CD5^+CD1d^+$ B cells (Breg), $IL\text{-}10^+CD19^+B220^+CD5^+CD1d^+$ B cells ($IL\text{-}10^+$ Breg), $CD19^-CD138^+$ B cells (plasma cells), and $CD19^+CD95^+GL7^+$ B cells (GC B cells) obtained from the SMGs (from four mice in each group), respectively. (e) Quantitative analysis of Breg, $IL\text{-}10^+$ Breg, plasma cells, and GC B cells. Throughout, data are presented by mean ± SD *, $p < 0.05$, **, $p < 0.01$, ***, $p < 0.001$. Statistical analyses were performed using one-way ANOVA.

and S7). The strong correlation of impaired Treg frequency with the breakdown of immune tolerance, the emergence of autoreactive immune cells, and the progression of SS has been demonstrated.[3,52] Several mechanisms of Treg-mediated immune homeostasis have been verified. Briefly, curbing excessive immune cell activations, secreting of immunosuppressive cytokines, and maintaining immune homeostasis are involved.[53] Treg deficiency or depletion leads to autoimmune diseases.[54] However, the mice treated with tFNAs showed significant restoration in the frequency of Tregs (Figure 4a, Figures S6 and S7), which to a large extent was relevant to the inhibition of SS disease progress. In the treatment of SS, inducing regulatory immune cells to inhibit autoreactive immune cells and halt the disease progression is an exceptionally promising immunotherapy.[55]

Additionally, the loss of balance between Th1 and Th2 is known to promote the development of the disease. We showed that, although tFNA treatment did not increase the frequency of Th2 cells, it suppressed the percentage of Th1 cells, hence helping with the recovery of Th1/Th2 equipoise (Figure 4b, Figures S6–S8). As IL-17-producing T cells, a large number of Th17 cells get involved in SS (Figure 4c, Figures S6 and S7).

https://doi.org/10.1021/acsami.1c14861
ACS Appl. Mater. Interfaces 2021, 13, 42543–42553

We found that tFNA treatment remarkably decreased the frequency of Th17 cells. Being a particular subgroup of $CD4^+$ T cells, Tfh cells are specialized in offering help to B cells. The proportion of Tfh cells in the NOD + saline group increased significantly compared with that in the normal mouse group (Figure 4d, Figure S6). After four weeks of tFNA treatment, the Tfh cell proportion declined remarkably, almost returning back to normal status compared to the normal mouse group. To sum up, all these results demonstrated the immune regulatory effects of tFNA therapy, which favored Treg differentiation while inhibiting Th1, Th17, and Tfh responses.

The mechanisms of inducing Tregs remained complicated. In our study, we attempted to find out possible mechanisms of the tFNA treatment inducing Tregs. Tregs can be produced in central and peripheral immune organs. During the Treg differentiation in the periphery, three signals are indispensably required, including the TCR signal (signal 1), costimulatory molecules (signal 2), and cytokines (signal 3).[56] In signal 3, different cytokines dictate the different differentiation programs of naïve $CD4^+$ T cells in the peripheral. Among various cytokines, TGF-β and IL-10 are considered to facilitate the induction of Tregs in the differentiation program.[57] In our study, tFNA treatment altered cytokines in the peripheral organs. The levels of TGF-β and IL-10 in the SMGs and the blood were increased, which may promote naive $CD4^+$ T cells to differentiate to Tregs in the periphery.

3.5. tFNAs Regulate B-Cell Differentiation. The alteration of B cells and cytokines produced by B cells was also observed. B cells and their cytokines infiltrating the SMGs were detected by immunofluorescence analysis. B cells are characterized by high expression of CD19. The frequency of CD19 positive cells was remarkably less in tFNA-treated groups compared with the NOD + saline group (Figure 5a, c). BAFF, a key cytokine for differentiation, proliferation, and survival of B cells, was measured in the SMGs by immunofluorescence analysis. After tFNA treatment, a decrease in the level of BAFF was observed, in accordance with the decline in the frequency of B cells in the SMGs (Figure 5b).

B cell subpopulations in the spleen and the SMGs were further investigated by multicolor flow cytometry. Similar to Tregs, Bregs are immunoregulatory cells that contribute to the maintenance of immune tolerance as well. We evaluated the effect of tFNA therapy on the differentiation of Bregs, which were referred to here as $CD19^+B220^+CD5^+CD1d^+$ B cells. We found that in the NOD + T250 group, the frequency of $CD19^+B220^+CD5^+CD1d^+$ Bregs were at normal status (Figure 5d, e, Figures S9 and 10). $CD19^+B220^+CD5^+CD1d^+IL\text{-}10^+$ B cells were regarded as B cells with regulatory capacity. Compared to the NOD + saline group, the frequency of these cells in the NOD + T250 group was greatly restored (Figure 5d, e, Figures S9 and 10). Interestingly, there was a marked reduction in the frequency of $CD19^-CD139^+$ plasma cells and $CD19^+CD95^+GL7^+$ germinal center (GC) B cells in the SMGs, the spleen, and the PB of the NOD + T250 group (Figure 5d, e, Figures S9 and 10). The differentiation of plasma cells was hindered under the control of GC B cells.[12] The alterations of plasma cells, GC B cells, and T cells were agreeable in our study. Taken together, these results demonstrated that tFNA treatment concurrently increased the frequency of Bregs and limited GC B cell and plasma cell differentiation.

Apart from T cells, B cells also play a non-negligible role in SS. Given the fact that the effect of tFNA treatment on altering T cells have already been demonstrated, B cell responses should also be monitored. The overactive T and B cells both infiltrate the SMGs in SS. $CD4^+$ T cells are regarded as the early infiltrating lymphocytes in SMGs, whereas B cells show up at a later stage. The interaction between $CD4^+$ T and B cells results in persistent inflammation, leading to the loss of normal structure and secretory function of SG. Before the onset of inflammation in SG, ectopic GC occurs in SG. GC is also found in human and animal models of SS. GC formation represents a key character of B cell hyperactivity as well as another histologic feature of SS.[12] The number of GC in SG is related to the degree of inflammation. In GC, $CD19^+CD95^+GL7^+$B cells were regarded as GC B cells.[58] With the help of Tfh cells, GC B cells can differentiate into either memory B cells or plasma cells in GC.[58] After the SS mice treated with 250 nM tFNAs, the frequencies of both GC B cells and plasma cells significantly decreased. We speculate that the number of GC also declined in that group, which corresponded to the suppression of overall inflammation in our study. Different to GC B cells and plasma cells, Bregs were considered to impose negative regulatory effect and could inhibit effector cell subsets, including monocytes, dendritic cells, Th1, Th17, Tfh cells and $CD8^+$ T cells. In addition, Bregs could stimulate the differentiation of Tregs.[12] Defects in Breg function have been demonstrated in numerous animal models of autoimmune diseases and patients with autoimmune diseases. It is highly possible that upregulation of the frequency and recovery of the function of Bregs are the potential therapeutic targets for autoimmune diseases.[59] Collectively, the results indicated that tFNA treatment selectively increased the frequency of Bregs and supported Breg function. Thus, we achieved comparable results in T cell and B cell measurements.

To find out the optimal concentration of tFNA treatment, 250 and 500 nM tFNAs were employed in our experiment. According to the protocol of tFNAs, tFNAs at low concentrations (normally < 250 nM) have no obvious cytotoxicity or adverse effects on living cells in vitro studies.[60] The concentration-dependent manner from 62.5 to 250 nM was utilized to find out the optimal dose of tFNAs in the previous studies of our research team.[37,42,61−64] Amazingly, 250 nM tFNAs showed the strongest effect on the promotions of cell proliferation and migration all the time. In vivo, 250 nM was employed as the only concentration of tFNAs in the studies and worked well.[42,63] Therefore, 250 nM tFNAs was the first choice in our study. However, a recent study found that local injection of 500 nM tFNAs showed better effects on anti-inflammation and tissue regeneration in periodontitis treatment, compared with 250 nM tFNAs.[40] Therefore, 500 nM tFNAs was added in our study. In our experiment, 250 nM tFNAs successfully restored saliva secretion, reversing SS, by inducing immune tolerance. The therapeutic effects of 500 nM tFNAs were not as satisfying as those of 250 nM tFNAs. In our view, the unsatisfied effects of 500 nM tFNAs might be due to the relatively high concentration. Different from local injection, the concentration of 500 nM was too high to be utilized to inject systemically.

Our study demonstrated the immunoregulatory capabilities of tFNA. Recently, reviews nominated various kinds of materials used in immunotherapy,[21,22] including macromaterials, micromaterials, and in particular, nanomaterials. However, no framework nucleic acids were mentioned in these

https://doi.org/10.1021/acsami.1c14861
ACS Appl. Mater. Interfaces 2021, 13, 42543−42553

reviews. Moreover, the therapeutic materials in the reviews served as vehicles. They do not have immunoregulatory capabilities themselves. Our study verified the viability, security, and availability in the treatment of autoimmune disease via regulating the immune system (Figure S11). Therefore, our study not only introduces an unprecedented nanomaterial for immunotherapy but also demonstrates that tFNAs regulate the immune system by themselves. Notably, similar to other nanomaterials, tFNAs are frequently considered to be superior drug carriers.[36,65−69] It can be imagined that a nanomaterial with great immune regulatory and delivery capabilities will be a promising candidate for the immunotherapy of autoimmune diseases in the near future.

4. CONCLUSION

In conclusion, our study indicates, for the first time, that tFNA injection is a safe and effective treatment for SS in NOD mice. tFNA treatment greatly inhibited local and systematic inflammation to halt the progression of SS and help restore saliva secretion. Through monitoring of T and B cell responses, tFNA treatment selectively reduces overactive T and B cells, including Th1, Th17, Tfh, GC B cells, and plasma cells, while inducing regulatory cells, without overall immunosuppression. In our study, tFNAs were applied in the SS immunotherapy and their immunoregulatory capabilities were confirmed. Previously, tFNAs were also proved to be superior drug carriers. Thus, our study has a profound implication for future scientific research using tFNAs as a promising treatment option for patients with SS and other autoimmune diseases.

■ ASSOCIATED CONTENT

Supporting Information

The Supporting Information is available free of charge at https://pubs.acs.org/doi/10.1021/acsami.1c14861.

Figure S1, AFM image of tFNAs; Figure S2, blood cytokine concentration at the end point of the experiment; Figure S3−S5, representative immunofluorescence images of SMGs; Figure S6−S7, representative flow cytometry pattern and quantitative analyses of $CD4^+$ T cell subsets; Figure S8, quantitative analysis of Th2 in SMGs; Figures S9 and S10, representative flow cytometry pattern and quantitative analyses of B cell subsets; Figure S11, representative histological images of heart, liver, lung, and kidney (PDF)

■ AUTHOR INFORMATION

Corresponding Authors

Xiaoxiao Cai − *State Key Laboratory of Oral Diseases, West China Hospital of Stomatology, Sichuan University, Chengdu 610041, China;* orcid.org/0000-0002-5654-7414; Email: xcai@scu.edu.cn

Yu Chen − *State Key Laboratory of Oral Diseases, West China Hospital of Stomatology, Sichuan University, Chengdu 610041, China*; Email: chen_yu55@hotmail.com

Authors

Shaojingya Gao − *State Key Laboratory of Oral Diseases, West China Hospital of Stomatology, Sichuan University, Chengdu 610041, China*

Yun Wang − *State Key Laboratory of Oral Diseases, West China Hospital of Stomatology, Sichuan University, Chengdu 610041, China*

Yanjing Li − *State Key Laboratory of Oral Diseases, West China Hospital of Stomatology, Sichuan University, Chengdu 610041, China*

Dexuan Xiao − *State Key Laboratory of Oral Diseases, West China Hospital of Stomatology, Sichuan University, Chengdu 610041, China*

Yunfeng Lin − *State Key Laboratory of Oral Diseases, West China Hospital of Stomatology, Sichuan University, Chengdu 610041, China; College of Biomedical Engineering, Sichuan University, Chengdu 610041, China;* orcid.org/0000-0003-1224-6561

Complete contact information is available at: https://pubs.acs.org/10.1021/acsami.1c14861

Author Contributions

S.G. and Y.W. contributed equally to this work. X.C., Y.C., S.G., and Y.W. conceived this project. X.C., Y.C., S.G., Y.W., and Y.L. designed the project and collected the data. S.G. analyzed the data and wrote the manuscript. Y.L., D.X., Y.Y., and Y.G. provided help during data collection. Y.W. and Y.L. provided writing assistance and helped during proofreading of the article.

Author Contributions

†S.G. and Y.W. contributed equally to this work.

Notes

The authors declare no competing financial interest.

■ ACKNOWLEDGMENTS

This study was supported by This study was supported by National Key R&D Program of China (2019YFA0110600) and National Natural Science Foundation of China (81970986, 81771125).

■ ABBREVIATIONS

SS, Sjogren's syndrome; tFNAs, tetrahedral framework nucleic acids; NOD mice, non-obese diabetic mice; SMG, submandibular glands; Tregs, regulatory T cells; Th1, T helper 1; Th17, T helper 17; Tfh, follicular helper T; GC, germinal center; SG, salivary glands; PB, peripheral blood; Bregs, regulatory B cells; 3D, three-dimensional; ssDNAs, single-stranded DNAs; PAGE, polyacrylamide gel electrophoresis; HPCE, high-performance capillary electrophoresis; AFM, atomic force microscopy; TEM, transmission electron microscopy; SPR, saliva flow rate; H&E, hematoxylin and eosin; TUNEL, TdT-mediated dUTP nick-end labeling; ELISA, enzyme-linked immunosorbent assay; ANOVA, analysis of variance; α-SMA, alpha smooth muscle actin; CK5, cytokeratin 5; AQP, aquaporins; Foxp3, factor forkhead box P3.

■ REFERENCES

(1) Fox, R. I. Sjögren's Syndrome. *Lancet* **2005**, *366* (9482), 321−331.

(2) Sandhya, P.; Kurien, B. T.; Danda, D.; Scofield, R. H. Update on Pathogenesis of Sjogren's Syndrome. *Curr. Rheumatol. Rev.* **2017**, *13* (1), 5−22.

(3) Katsifis, G. E.; Moutsopoulos, N. M.; Wahl, S. M. T lymphocytes in Sjogren's Syndrome: Contributors to and Regulators of Pathophysiology. *Clin. Rev. Allergy Immunol.* **2007**, *32* (3), 252−264.

(4) Psianou, K.; Panagoulias, I.; Papanastasiou, A. D.; de Lastic, A. L.; Rodi, M.; Spantidea, P. I.; Degn, S. E.; Georgiou, P.; Mouzaki, A. Clinical and Immunological Parameters of Sjogren's Syndrome. *Autoimmun. Rev.* **2018**, *17* (10), 1053−1064.

(5) Saccucci, M.; Di Carlo, G.; Bossu, M.; Giovarruscio, F.; Salucci, A.; Polimeni, A. Autoimmune Diseases and Their Manifestations on Oral Cavity: Diagnosis and Clinical Management. *J. Immunol. Res.* **2018**, *2018*, 6061825.
(6) Fernández-Martínez, G.; Zamora-Legoff, V.; Hernández Molina, G. Oral Health-related Quality of Life in Primary Sjögren's Syndrome. *Reumatología Clínica (English Edition)* **2020**, *16* (2), 92−96.
(7) Rusthen, S.; Young, A.; Herlofson, B. B.; Aqrawi, L. A.; Rykke, M.; Hove, L. H.; Palm, O.; Jensen, J. L.; Singh, P. B. Oral Disorders, Saliva Secretion, and Oral Health-related Quality of Life in Patients with Primary Sjogren's Syndrome. *Eur. J. Oral Sci.* **2017**, *125* (4), 265−271.
(8) Guisado-Vasco, P.; Silva, M.; Duarte-Millan, M. A.; Sambataro, G.; Bertolazzi, C.; Pavone, M.; Martin-Garrido, I.; Martin-Segarra, O.; Luque-Pinilla, J. M.; Santilli, D.; Sambataro, D.; Torrisi, S. E.; Vancheri, A.; Gutierrez, M.; Mejia, M.; Palmucci, S.; Mozzani, F.; Rojas-Serrano, J.; Vanchieri, C.; Sverzellati, N.; Ariani, A. Quantitative Assessment of Interstitial Lung Disease in Sjogren's Syndrome. *PLoS One* **2019**, *14* (11), No. e0224772.
(9) Saraux, A.; Pers, J. O.; Devauchelle-Pensec, V. Treatment of Primary Sjogren Syndrome. *Nat. Rev. Rheumatol.* **2016**, *12* (8), 456−71.
(10) Seror, R.; Mariette, X. Guidelines for Treatment of Primary Sjogren's Syndrome: a First Useful Stone But Still Much to Do. *Rheumatology (Oxford, U. K.)* **2017**, *56* (10), 1641−1642.
(11) Garber, K. Immunology: A Tolerant Approach. *Nature* **2014**, *507*, 418−420.
(12) Nocturne, G.; Mariette, X. B cells in the Pathogenesis of Primary Sjogren Syndrome. *Nat. Rev. Rheumatol.* **2018**, *14* (3), 133−145.
(13) Tzioufas, A. G.; Kapsogeorgou, E. K.; Moutsopoulos, H. M. Pathogenesis of Sjogren's Syndrome: What We Know and What We Should Learn. *J. Autoimmun.* **2012**, *39* (1−2), 4−8.
(14) van Woerkom, J. M.; Kruize, A. A.; Wenting-van Wijk, M. J.; Knol, E.; Bihari, I. C.; Jacobs, J. W.; Bijlsma, J. W.; Lafeber, F. P.; van Roon, J. A. Salivary Gland and Peripheral Blood T helper 1 and 2 Cell Activity in Sjogren's Syndrome Compared with Non-Sjogren's Sicca Syndrome. *Ann. Rheum. Dis.* **2005**, *64* (10), 1474−9.
(15) Du, Z. H.; Ding, C.; Zhang, Q.; Zhang, Y.; Ge, X. Y.; Li, S. L.; Yu, G. Y. Stem Cells from Exfoliated Deciduous Teeth Alleviate Hyposalivation Caused by Sjogren Syndrome. *Oral Dis* **2019**, *25* (6), 1530−1544.
(16) Alunno, A.; Carubbi, F.; Bistoni, O.; Caterbi, S.; Bartoloni, E.; Mirabelli, G.; Cannarile, F.; Cipriani, P.; Giacomelli, R.; Gerli, R. T Regulatory and T Helper 17 Cells in Primary Sjogren's Syndrome: Facts and Perspectives. *Mediators Inflammation* **2015**, *2015*, 243723.
(17) Murphy, K. M.; Reiner, S. L. The Lineage Decisions of Helper T cells. *Nat. Rev. Immunol.* **2002**, *2* (12), 933−44.
(18) Quan, S.; Sheng, J. R.; Abraham, P. M.; Soliven, B. Regulatory T and B Lymphocytes in a Spontaneous Autoimmune Polyneuropathy. *Clin. Exp. Immunol.* **2016**, *184* (1), 50−61.
(19) Xu, J.; Wang, D.; Liu, D.; Fan, Z.; Zhang, H.; Liu, O.; Ding, G.; Gao, R.; Zhang, C.; Ding, Y.; Bromberg, J. S.; Chen, W.; Sun, L.; Wang, S. Allogeneic Mesenchymal Stem Cell Treatment Alleviates Experimental and Clinical Sjogren Syndrome. *Blood* **2012**, *120* (15), 3142−51.
(20) Jin-Sil, P.; Sun-Hee, H.; SeungCheon, Y.; JeongWon, C.; Kyung-Ah, J.; Mi-La, C.; Sung-Hwan, P. Immune Modulation by Rebamipide in a Mouse Model of Sjogren's Syndrome via T and B cell Regulation. *Immunol. Lett.* **2019**, *214*, 1−7.
(21) Eppler, H. B.; Jewell, C. M. Biomaterials as Tools to Decode Immunity. *Adv. Mater.* **2020**, *32* (13), No. e1903367.
(22) Shields, C. W. t.; Wang, L. L.; Evans, M. A.; Mitragotri, S. Materials for Immunotherapy. *Adv. Mater.* **2020**, *32* (13), No. e1901633.
(23) Kishimoto, T. K.; Maldonado, R. A. Nanoparticles for the Induction of Antigen-Specific Immunological Tolerance. *Front. Immunol.* **2018**, *9*, 230.
(24) Singha, S.; Shao, K.; Ellestad, K. K.; Yang, Y.; Santamaria, P. Nanoparticles for Immune Stimulation Against Infection, Cancer, and Autoimmunity. *ACS Nano* **2018**, *12* (11), 10621−10635.
(25) Ji, X.; Guo, D.; Ma, J.; Yin, M.; Yu, Y.; Liu, C.; Zhou, Y.; Sun, J.; Li, Q.; Chen, N.; Fan, C.; Song, H. Epigenetic Remodeling Hydrogel Patches for Multidrug-Resistant Triple-Negative Breast Cancer. *Adv. Mater.* **2021**, *33* (18), No. e2100949.
(26) Sun, W.; Ji, W.; Hu, Q.; Yu, J.; Wang, C.; Qian, C.; Hochu, G.; Gu, Z. Transformable DNA Nanocarriers for Plasma Membrane Targeted Delivery of Cytokine. *Biomaterials* **2016**, *96*, 1−10.
(27) Nishikawa, M.; Ogawa, K.; Umeki, Y.; Mohri, K.; Kawasaki, Y.; Watanabe, H.; Takahashi, N.; Kusuki, E.; Takahashi, R.; Takahashi, Y.; Takakura, Y. Injectable, Self-gelling, Biodegradable, and Immunomodulatory DNA Hydrogel for Antigen Delivery. *J. Controlled Release* **2014**, *180*, 25−32.
(28) Auvinen, H.; Zhang, H.; Nonappa; Kopilow, A.; Niemela, E. H.; Nummelin, S.; Correia, A.; Santos, H. A.; Linko, V.; Kostiainen, M. A. Protein Coating of DNA Nanostructures for Enhanced Stability and Immunocompatibility. *Adv. Healthcare Mater.* **2017**, *6* (18), 1700692.
(29) Zhang, X.; Kang, Y.; Wang, J.; Yan, J.; Chen, Q.; Cheng, H.; Huang, P.; Gu, Z. Engineered PD-L1-Expressing Platelets Reverse New-Onset Type 1 Diabetes. *Adv. Mater.* **2020**, *32* (26), No. e1907692.
(30) Liu, Q.; Wang, X.; Liu, X.; Kumar, S.; Gochman, G.; Ji, Y.; Liao, Y. P.; Chang, C. H.; Situ, W.; Lu, J.; Jiang, J.; Mei, K. C.; Meng, H.; Xia, T.; Nel, A. E. Use of Polymeric Nanoparticle Platform Targeting the Liver To Induce Treg-Mediated Antigen-Specific Immune Tolerance in a Pulmonary Allergen Sensitization Model. *ACS Nano* **2019**, *13* (4), 4778−4794.
(31) Liu, C.; Zhou, Y. F.; Ji, X. Y.; Xie, H.; Hu, X. J.; Yin, M.; Chen, N.; Fan, C. H.; Song, H. Y. Nanobooster-encapsulated Dybrid RNA as Anti-tumor Viral Mimicry. *Nano Today* **2021**, *38*, 101211.
(32) Fu, W.; Ma, L.; Ju, Y.; Xu, J. G.; Li, H.; Shi, S. R.; Zhang, T.; Zhou, R. H.; Zhu, J. W.; Xu, R. X.; You, C.; Lin, Y. F. Therapeutic siCCR2 Loaded by Tetrahedral Framework DNA Nanorobotics in Therapy for Intracranial Hemorrhage. *Adv. Funct. Mater.* **2021**, *31* (33), 2101435.
(33) Li, J. J.; Xiao, L. R.; Yan, N. H.; Li, Y. J.; Wang, Y.; Qin, X.; Zhao, D.; Liu, M. T.; Li, N.; Lin, Y. F. The Neuroprotective Effect of MicroRNA-22−3p Modified Tetrahedral Framework Nucleic Acids on Damaged Retinal Neurons Via TrkB/BDNF Signaling Pathway. *Adv. Funct. Mater.* **2021**, 2104141.
(34) Cui, W. T.; Yang, X.; Chen, X. Y.; Xiao, D. X.; Zhu, J. Y.; Zhang, M.; Qin, X.; Ma, X. H.; Lin, Y. F. Treating LRRK2-Related Parkinson's Disease by Inhibiting the mTOR Signaling Pathway to Restore Autophagy. *Adv. Funct. Mater.* **2021**, 2105152.
(35) Sirong, S.; Yang, C.; Taoran, T.; Songhang, L.; Shiyu, L.; Yuxin, Z.; Xiaoru, S.; Tao, Z.; Yunfeng, L.; Xiaoxiao, C. Effects of Tetrahedral Framework Nucleic Acid/Wogonin Complexes on Osteoarthritis. *Bone Res.* **2020**, *8*, 6.
(36) Tian, T.; Xiao, D.; Zhang, T.; Li, Y.; Shi, S.; Zhong, W.; Gong, P.; Liu, Z.; Li, Q.; Lin, Y. A Framework Nucleic Acid Based Robotic Nanobee for Active Targeting Therapy. *Adv. Funct. Mater.* **2021**, *31* (5), 2007342.
(37) Zhang, Q.; Lin, S.; Shi, S.; Zhang, T.; Ma, Q.; Tian, T.; Zhou, T.; Cai, X.; Lin, Y. Anti-inflammatory and Antioxidative Effects of Tetrahedral DNA Nanostructures via the Modulation of Macrophage Responses. *ACS Appl. Mater. Interfaces* **2018**, *10* (4), 3421−3430.
(38) Yang, Y.; Zhu, J.; Ma, W.; Zhang, W.; Xie, Y.; Chen, X.; Zhu, J.; Liu, Y.; Qin, X.; Lin, Y. The Remyelination Effect of DNA Framework Nucleic Acids on Demyelinating Diseases. *Applied Materials Today* **2021**, *24*, 101098.
(39) Zhu, J.; Zhang, M.; Gao, Y.; Qin, X.; Zhang, T.; Cui, W.; Mao, C.; Xiao, D.; Lin, Y. Tetrahedral Framework Nucleic Acids Promote Scarless Healing of Cutaneous Wounds via the AKT-signaling Pathway. *Signal Transduct Target Ther* **2020**, *5* (1), 120.
(40) Zhou, M.; Gao, S.; Zhang, X.; Zhang, T.; Zhang, T.; Tian, T.; Li, S.; Lin, Y.; Cai, X. The Protective Effect of Tetrahedral Framework

https://doi.org/10.1021/acsami.1c14861
ACS Appl. Mater. Interfaces 2021, 13, 42543−42553

Nucleic Acids on Periodontium under Inflammatory Conditions. *Bioact Mater.* **2021**, *6* (6), 1676−1688.
(41) Sun, Y.; Liu, Y.; Zhang, B.; Shi, S.; Zhang, T.; Zhao, D.; Tian, T.; Li, Q.; Lin, Y. Erythromycin Loaded by Tetrahedral Framework Nucleic Acids Are More Antimicrobial Sensitive Against Escherichia Coli (E. coli). *Bioact Mater.* **2021**, *6* (8), 2281−2290.
(42) Lin, S.; Zhang, Q.; Li, S.; Zhang, T.; Wang, L.; Qin, X.; Zhang, M.; Shi, S.; Cai, X. Antioxidative and Angiogenesis-Promoting Effects of Tetrahedral Framework Nucleic Acids in Diabetic Wound Healing with Activation of the Akt/Nrf2/HO-1 Pathway. *ACS Appl. Mater. Interfaces* **2020**, *12* (10), 11397−11408.
(43) Braley-Mullen, H.; Yu, S. NOD.H-2h4Mice: an Important and Underutilized Animal Model of Autoimmune Thyroiditis and Sjogren's Syndrome. *Adv. Immunol.* **2015**, *126*, 1−43.
(44) Scuron, M. D.; Fay, B.; Oliver, J.; Smith, P. Spontaneous Model of Sjogren's Syndrome in NOD Mice. *Curr. Protoc Pharmacol* **2019**, *86* (1), e65.
(45) Soyfoo, M. S.; Chivasso, C.; Perret, J.; Delporte, C. Involvement of Aquaporins in the Pathogenesis, Diagnosis and Treatment of Sjogren's Syndrome. *Int. J. Mol. Sci.* **2018**, *19* (11), 3392.
(46) Delporte, C. Aquaporins in Secretory Glands and Their Role in Sjögren's Syndrome. *Handb Exp Pharmacol* **2009**, *190*, 185.
(47) Soyfoo, M. S.; Konno, A.; Bolaky, N.; Oak, J. S.; Fruman, D.; Nicaise, C.; Takiguchi, M.; Delporte, C. Link Between Inflammation and Aquaporin-5 Distribution in Submandibular Gland in Sjogren's Syndrome? *Oral Dis* **2012**, *18* (6), 568−74.
(48) Verstappen, G. M.; Kroese, F. G. M.; Bootsma, H. T cells in Primary Sjogren's Syndrome: Targets for Early Intervention. *Rheumatology (Oxford, U. K.)* **2021**, *60* (7), 3088.
(49) Rios-Rios, W. J.; Sosa-Luis, S. A.; Torres-Aguilar, H. T Cells Subsets in the Immunopathology and Treatment of Sjogren's Syndrome. *Biomolecules* **2020**, *10* (11), 1539.
(50) van Beers, J.; Damoiseaux, J. Immune Monitoring upon Treatment with Biologics in Sjogren's Syndrome: The What, Where, When, and How. *Biomolecules* **2021**, *11* (1), 116.
(51) Kanamori, M.; Nakatsukasa, H.; Okada, M.; Lu, Q.; Yoshimura, A. Induced Regulatory T Cells: Their Development, Stability, and Applications. *Trends Immunol.* **2016**, *37* (11), 803−811.
(52) Martinez Allo, V. C.; Hauk, V.; Sarbia, N.; Pinto, N. A.; Croci, D. O.; Dalotto-Moreno, T.; Morales, R. M.; Gatto, S. G.; Manselle Cocco, M. N.; Stupirski, J. C.; Deladoey, A.; Maronna, E.; Marcaida, P.; Durigan, V.; Secco, A.; Mamani, M.; Dos Santos, A.; Catalan Pellet, A.; Perez Leiros, C.; Rabinovich, G. A.; Toscano, M. A. Suppression of Age-related Salivary Gland Autoimmunity by Glycosylation-dependent Galectin-1-driven Immune Inhibitory Circuits. *Proc. Natl. Acad. Sci. U. S. A.* **2020**, *117* (12), 6630−6639.
(53) Ferreira, L. M. R.; Muller, Y. D.; Bluestone, J. A.; Tang, Q. Next-generation Regulatory T cell Therapy. *Nat. Rev. Drug Discovery* **2019**, *18* (10), 749−769.
(54) Dominguez-Villar, M.; Hafler, D. A. Regulatory T cells in Autoimmune Disease. *Nat. Immunol.* **2018**, *19* (7), 665−673.
(55) Sharabi, A.; Tsokos, M. G.; Ding, Y.; Malek, T. R.; Klatzmann, D.; Tsokos, G. C. Regulatory T cells in the Treatment of Disease. *Nat. Rev. Drug Discovery* **2018**, *17* (11), 823−844.
(56) Curtsinger, J. M.; Lins, D. C.; Mescher, M. F. Signal 3 Determines Tolerance Versus Full Activation of Naive CD8 T cells: Dissociating Proliferation and Development of Effector Function. *J. Exp. Med.* **2003**, *197* (9), 1141−51.
(57) Kalekar, L. A.; Mueller, D. L. Relationship between CD4 Regulatory T Cells and Anergy In Vivo. *J. Immunol.* **2017**, *198* (7), 2527−2533.
(58) Chen, W.; Yang, F.; Xu, G.; Ma, J.; Lin, J. Follicular Helper T cells and Follicular Regulatory T cells in the Immunopathology of Primary Sjogren's Syndrome. *J. Leukocyte Biol.* **2021**, *109* (2), 437−447.
(59) Wu, H.; Su, Z.; Barnie, P. A. The Role of B Regulatory (B10) Cells in Inflammatory Disorders and Their Potential as Therapeutic Targets. *Int. Immunopharmacol.* **2020**, *78*, 106111.
(60) Zhang, T.; Tian, T.; Zhou, R.; Li, S.; Ma, W.; Zhang, Y.; Liu, N.; Shi, S.; Li, Q.; Xie, X.; Ge, Y.; Liu, M.; Zhang, Q.; Lin, S.; Cai, X.; Lin, Y. Design, Fabrication and Applications of Tetrahedral DNA Nanostructure-based Multifunctional Complexes in Drug Delivery and Biomedical Treatment. *Nat. Protoc.* **2020**, *15* (8), 2728−2757.
(61) Zhao, D.; Cui, W.; Liu, M.; Li, J.; Sun, Y.; Shi, S.; Lin, S.; Lin, Y. Tetrahedral Framework Nucleic Acid Promotes the Treatment of Bisphosphonate-Related Osteonecrosis of the Jaws by Promoting Angiogenesis and M2 Polarization. *ACS Appl. Mater. Interfaces* **2020**, *12* (40), 44508−44522.
(62) Shi, S.; Lin, S.; Shao, X.; Li, Q.; Tao, Z.; Lin, Y. Modulation of Chondrocyte Motility by Tetrahedral DNA Nanostructures. *Cell Proliferation* **2017**, *50* (5), No. e12368.
(63) Liu, N.; Zhang, X.; Li, N.; Zhou, M.; Zhang, T.; Li, S.; Cai, X.; Ji, P.; Lin, Y. Tetrahedral Framework Nucleic Acids Promote Corneal Epithelial Wound Healing in Vitro and in Vivo. *Small* **2019**, *15* (31), No. e1901907.
(64) Mao, C.; Pan, W.; Shao, X.; Ma, W.; Zhang, Y.; Zhan, Y.; Gao, Y.; Lin, Y. The Clearance Effect of Tetrahedral DNA Nanostructures on Senescent Human Dermal Fibroblasts. *ACS Appl. Mater. Interfaces* **2019**, *11* (2), 1942−1950.
(65) Fu, W.; You, C.; Ma, L.; Li, H.; Ju, Y.; Guo, X.; Shi, S.; Zhang, T.; Zhou, R.; Lin, Y. Enhanced Efficacy of Temozolomide Loaded by a Tetrahedral Framework DNA Nanoparticle in the Therapy for Glioblastoma. *ACS Appl. Mater. Interfaces* **2019**, *11* (43), 39525−39533.
(66) Ge, Y.; Tian, T.; Shao, X.; Lin, S.; Zhang, T.; Lin, Y.; Cai, X. PEGylated Protamine-Based Adsorbing Improves the Biological Properties and Stability of Tetrahedral Framework Nucleic Acids. *ACS Appl. Mater. Interfaces* **2019**, *11* (31), 27588−27597.
(67) Li, S.; Sun, Y.; Tian, T.; Qin, X.; Lin, S.; Zhang, T.; Zhang, Q.; Zhou, M.; Zhang, X.; Zhou, Y.; Zhao, H.; Zhu, B.; Cai, X. MicroRNA-214−3p Modified Tetrahedral Framework Nucleic Acids Target Survivin to Induce Tumour Cell Apoptosis. *Cell Proliferation* **2020**, *53* (1), No. e12708.
(68) Liu, Y.; Sun, Y.; Li, S.; Liu, M.; Qin, X.; Chen, X.; Lin, Y. Tetrahedral Framework Nucleic Acids Deliver Antimicrobial Peptides with Improved Effects and Less Susceptibility to Bacterial Degradation. *Nano Lett.* **2020**, *20* (5), 3602−3610.
(69) Sun, Y.; Li, S.; Zhang, Y.; Li, Q.; Xie, X.; Zhao, D.; Tian, T.; Shi, S.; Meng, L.; Lin, Y. Tetrahedral Framework Nucleic Acids Loading Ampicillin Improve the Drug Susceptibility against Methicillin-Resistant Staphylococcus aureus. *ACS Appl. Mater. Interfaces* **2020**, *12* (33), 36957−36966.

https://doi.org/10.1021/acsami.1c14861
ACS Appl. Mater. Interfaces 2021, 13, 42543−42553